A STUDY OF THE FILLING OF HURRICANE DONNA (1960) OVER LAND

BANNER I. MILLER

National Hurricane Research Project, U.S. Weather Bureau, Miami, Fla.

ABSTRACT

The processes which resulted in the filling of a tropical cyclone over land have been investigated. The eddy fluxes of latent and sensible heat and the dissipation of kinetic energy at the earth's surface have been computed for a 3-day period. On the first two days the cyclone was over the ocean and on the third day it was over land. Hence it was possible to compare the rates of energy exchange at the surface after the character of the lower boundary had changed. Some significant differences in these rates of exchange were detected.

1. INTRODUCTION

The tropical cyclone is a thermally driven circulation in the direct sense. The role of the vertical flux of sensible and latent heat in both the formation and maintenance of tropical cyclones has been demonstrated by Palmén and Riehl [21] and by Malkus and Riehl [14]. The dissipation of kinetic energy by friction acts as a brake on hurricane development. Consequently, surface exchange processes are of fundamental importance to the hurricane mechanism.

As long as the tropical cyclone remains over the ocean where the water is warmer than the air, evaporation and the vertical flux of sensible heat from the ocean to the atmosphere contribute to the growth of the energy of the cyclone. Over land, tropical cyclones usually weaken rapidly. After a hurricane moves from a water surface to a land surface, the rate of frictional dissipation of kinetic energy at the lower boundary is assumed to change, but this has not been established. For many years it was believed that increased friction was the primary cause for the decay of hurricanes after landfall. Hubert [9] attempted to determine the effect of friction on the rate of filling after a hurricane passes from water to a land surface. He concluded that friction alone is not enough to account for the decrease in intensity over land, and suggested that a change in the available energy supply is the predominant factor which causes filling over land. Byers [2], Riehl [28], Bergeron [1], and Palmén [20] also believe that it is the removal of the sensible heat source (hence also the removal of the latent heat source) which makes the most important contribution to the filling process over land. However, no one has ever presented any calculations which support this hypothesis.

The purpose of this paper is to examine in detail the changes in the energy supply which occur after the center of a hurricane moves away from the warm waters of the tropical oceans. We shall examine the changes in the flux of energy through the lower boundary. This will include calculation of the vertical flux of both sensible and latent heat over water and over land. Frictional dissipation of kinetic energy over land and over water will be compared. Structural and thermodynamical changes observed during and after landfall will be related to the changes in the energy fluxes. The kinetic energy budget will also be computed, and it will be shown that the production of kinetic energy is less over land than it is over water. The reduction in the production of kinetic energy can also be related to the removal of the surface heat source. It is hoped that these calculations will partially answer the question as to whether filling of a tropical cyclone over land is due to increased friction or to the removal of the oceanic heat source.

2. SOURCES AND ANALYSES OF DATA

The calculations are based on data obtained in the vicinity of Hurricane Donna which occurred in September 1960. A portion of the track is shown in figure 1. Donna was selected because the center of the cyclone passed through a region where the density of rawinsonde stations is considerably greater than normal. The surface reporting stations in the Bahamas, Cuba, and Florida provided good data coverage at the surface, which was necessary for the computation of the energy exchanges between the lower boundary and the atmosphere. Research aircraft, flown by the Research Flight Facility of the Weather Bureau along paths near the core of the cyclone, collected detailed data on winds, temperatures, and relative humidities at three levels on September 9. The center of the cyclone was under constant radar surveillance for the entire period for which calculations were made. This made it easy to prepare a detailed track of hourly center positions which was necessary for determining the radial component of the wind. Another advantage in using the Donna data resulted from the fact that the thermal structure of the immediate environment of the cyclone remained almost constant

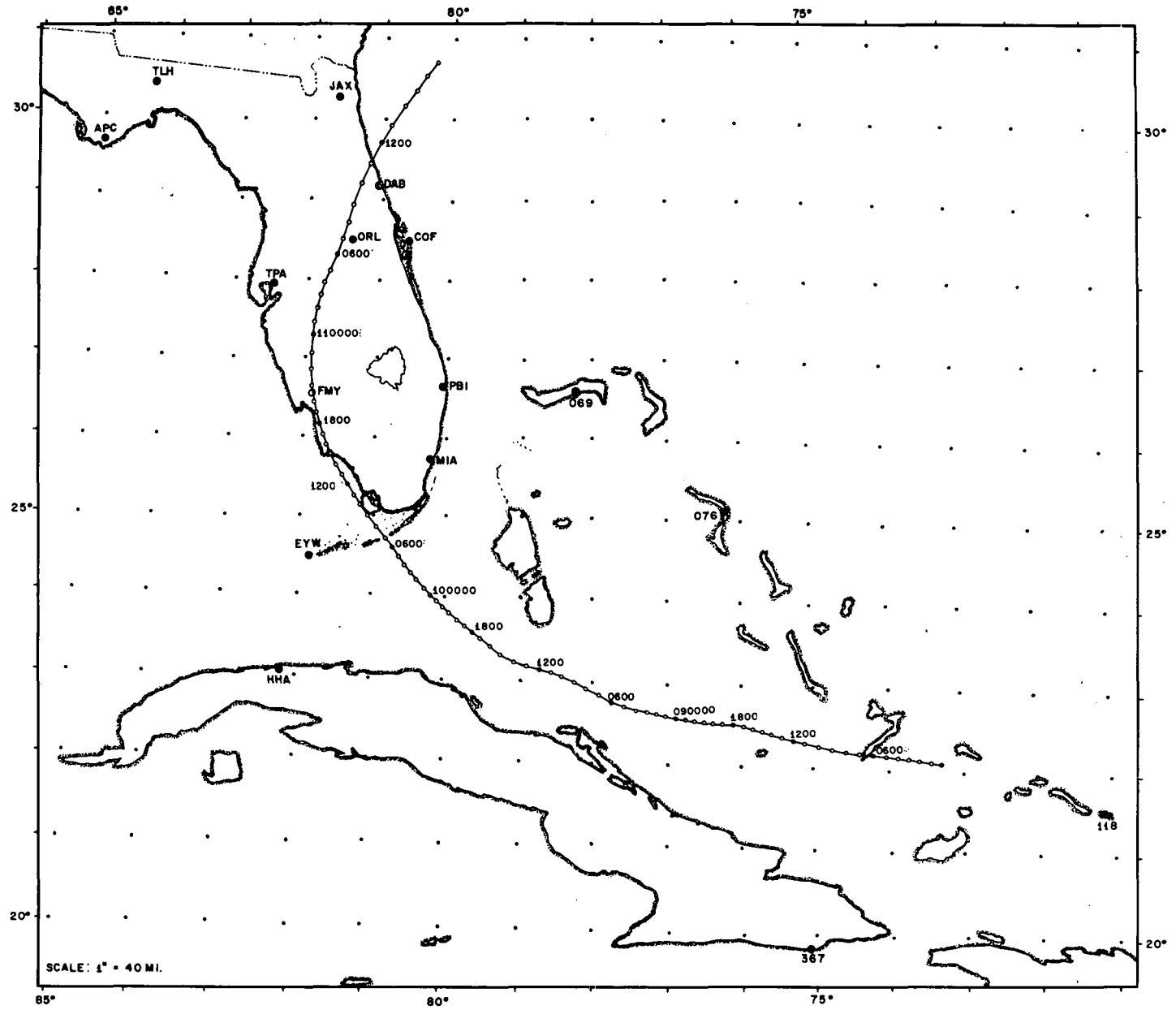

FIGURE 1.—Track of hurricane Donna, September 8–11, 1960. Time is GMT.

before and after the center of the cyclone moved inland over Florida. As a result, one could consider the Donna calculations as very nearly approaching a controlled experiment, in which the only variable allowed to change was the character of the lower boundary. Consequently, it provided an unusual opportunity to examine the effects of changed surface friction and surface heat source after the center of the hurricane moved inland.

The center of the hurricane passed north of Cuba on the 9th, across the Florida Keys on the 10th, and into central Florida during the early part of the 11th. Calculations were performed for each of these three days. On the 9th and 10th the center was over water and on the 11th the center was moving over land. The computations should, therefore, provide a basis for comparison of the energy transformations over water with those over land.

Many of the radiosonde stations made soundings at 3-hr. intervals when the center of the hurricane was less than 300 n. mi. away, and at 6-hr. intervals when the center was 300–800 n. mi. away. These data were supplemented by flight data collected by aircraft flying at 1600, 6400, and 14,200 ft. on the 9th. The tracks of these flights are shown in figure 2. Several dropsondes were made by the Navy from the 700-mb. level on the 9th and 10th. For any one synoptic time, however, the data were too sparse to permit the detailed calculations needed to describe the various energy transformations. Consequently, it was necessary to composite the available observations over 12-hr. periods in order to obtain enough data with which to work.

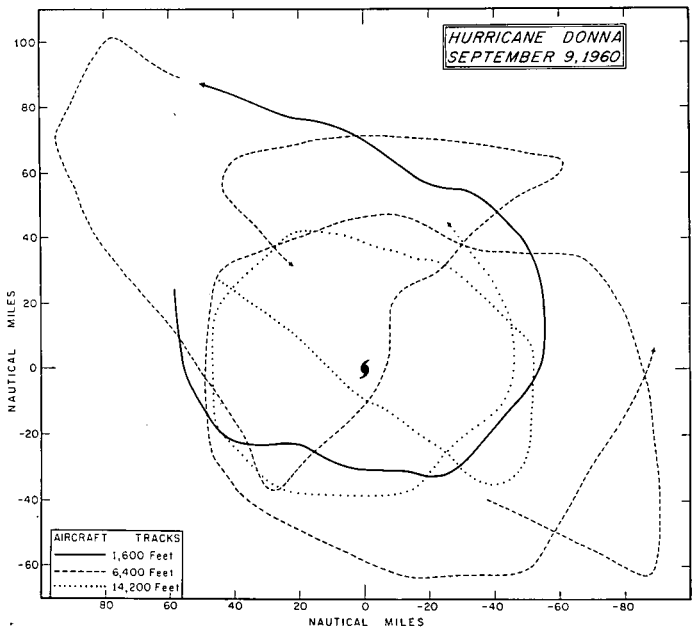

FIGURE 2.—Tracks of research aircraft at 1600, 6400, and 14,200 ft.

The three compositing periods included the hours from 0000 to 1200 GMT on the 9th, 10th, and 11th. The center was passing over land during these hours on the 11th. The same periods were selected on the 9th and 10th (while the center was over water) to eliminate the necessity for considering possible diurnal effects when over-water and over-land computations were compared.

The data were composited and plotted with respect to the center of the moving cyclone. At all levels, data were plotted at the actual position of the balloon at that level (in both space and time) rather than at the position of the observation station and at release time. The density of the data following the compositing process for the three 12-hr. periods is shown in figure 3.

The compositing of data around a tropical cyclone is necessary if one wishes to perform any sort of quantitative analyses. It is permissible as long as the cyclone is in a relatively steady state. On the 9th and 10th, Donna was probably as near to being in a steady state as a mature hurricane ever is. Hence, the compositing process gives a reasonably accurate picture of the cyclone. On the 11th, however, the center of the cyclone was moving over land, the central pressure was rising, and the circulation was weakening. This creates some doubt as to the validity of a composite chart. Figure 4 shows the time variations of the central pressure: It will be noted that most of the rise in the central pressure (more than 30 mb.) occurred between 1200 GMT on the 10th and 0000 GMT on the 11th. This gives some indication that the cyclone was in a quasi-steady state over land during the period for which data were composited. It would be preferable to have used only synoptic data, but this was impossible. In fact, no really complete synoptic description of the

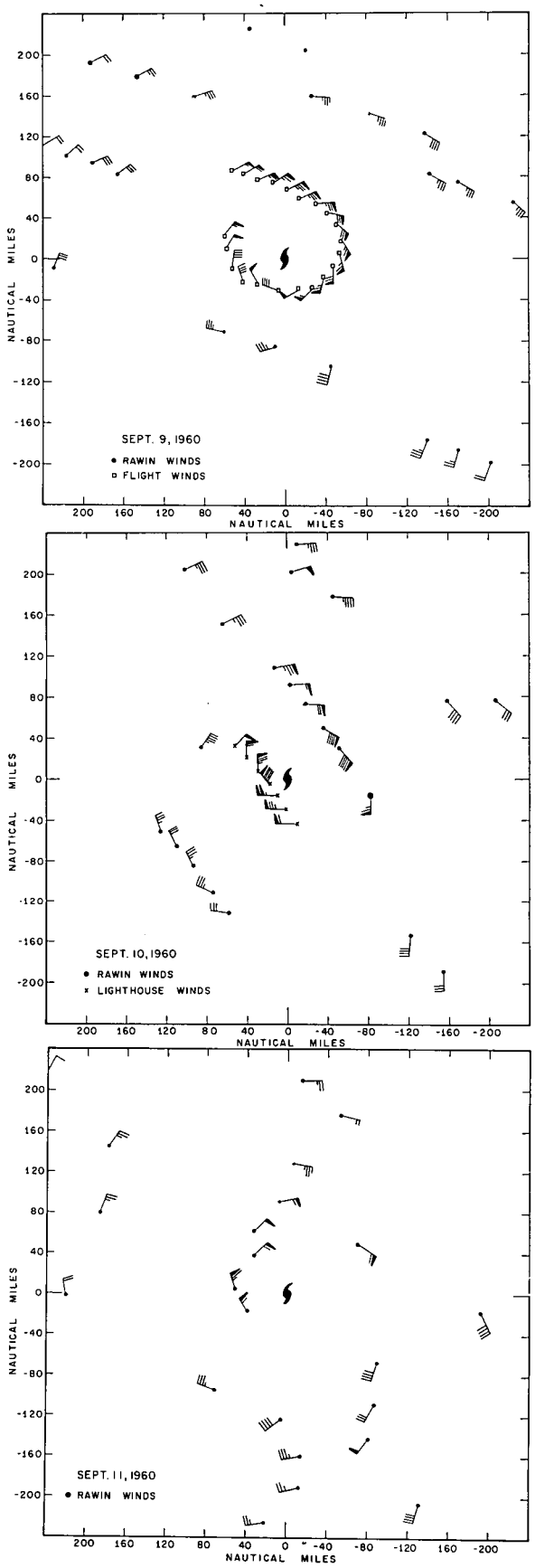

FIGURE 3.—Density of radiosonde, flight, and lighthouse data near hurricane Donna, September 9–11, 1960.

739-756—64——2

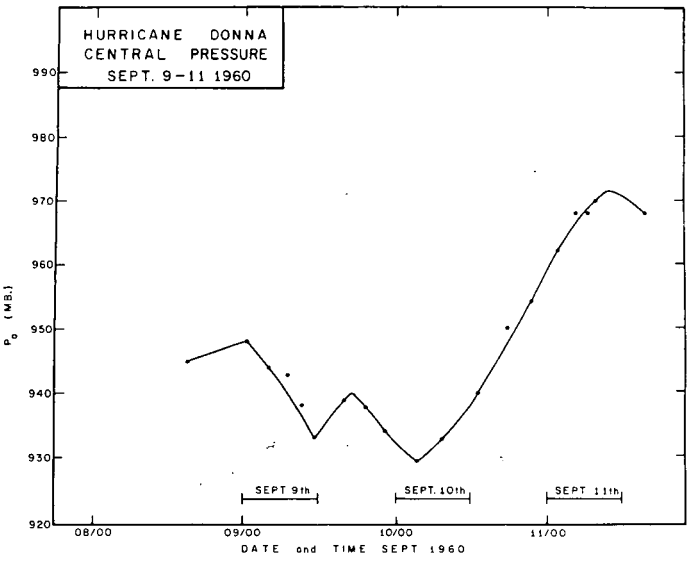

FIGURE 4.—Variations in central surface pressure with time, September 9–11, 1960. Time is GMT.

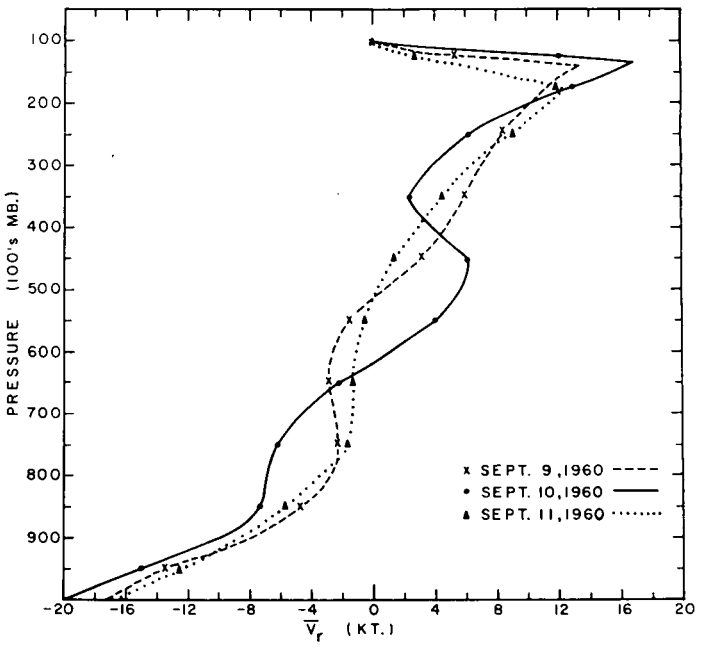

FIGURE 5.—Vertical profiles of the radial wind at 120-n. mi. radius.

inner portion of a tropical cyclone has ever been obtained. The nearest things are descriptions based on aircraft data obtained by the National Hurricane Research Project, but these data are also composited over periods of several hours.

Preparatory to analyzing the data, vertical profiles of wind speed and direction were plotted for the individual rawin soundings. Mean winds for layers of 100-mb. thickness from the surface up to 200 mb. were computed. For the 200–100-mb. layer, means were computed for 50-mb. increments. If the vertical variation of the wind direction through a layer was 20° or less, means were computed from the vertical profiles by equal-area methods. If the wind direction varied by more than 20°, means were computed from the balloon trajectory as recorded on the original rawin computation sheets. Most of the means for the layers above 300 mb. were computed from the balloon trajectory.

The mean layer winds were then composited with respect to the center of the cyclone. Radial and tangential components of both the actual and the relative winds were computed. These wind data, the heights of the constant pressure surfaces, the temperatures, and the mixing ratios (up to 250 mb.) were plotted at the middle of each layer (950, 850, . . ., 125 mb.) for each of the three compositing periods. The height field was carefully analyzed at each level. From the height analyses, thickness patterns were computed and these checked for thermal consistency. The thickness patterns were smoothed, where necessary, to make them fit the available temperature data. New height fields were then constructed by differential analysis. These new analyses were then compared with the originals and in most cases the difference was found to be negligible.

Perhaps the most important part of the analysis was the description of the radial mass flow which is of fundamental importance in explaining the energy transformations within the tropical cyclone. The rate of conversion of potential energy to kinetic energy depends upon the radial wind component. In hurricanes the minimum pressure is related to the mass flow (Kreuger [13]). Much of the latent heat energy is supplied by the radial transport of water vapor from the environment. Some radial transport of kinetic energy is apparently necessary to maintain the core of a steady-state tropical cyclone (Palmén and Riehl [21]; Rosenthal [30]). Integration of the kinetic energy equation over a cylindrical volume requires detailed knowledge of the mass flow inside the cylinder.

For the surface to 100-mb. layer there was only one common radius for which the mass flow could be accurately determined for all three days. This was the 120-n. mi. radius. For the middle of each layer (950, 850, . . ., 125 mb.) the radial wind component was plotted against azimuth. Where the 120-n. mi. radius fell between plotted data, the radial wind was obtained by linear interpolation of the mass flow. Smooth curves were drawn to fit the available data, and the radial wind was then read from the curves. These data were then adjusted for mass balance by setting

$$\oint\int_{p_0}^{p_t} v_r dp r d\theta = 0 \qquad (1)$$

where p_0 is the surface pressure, p_t is the pressure at the top of the cyclone (about 100 mb.), v_r is the radial wind, r is the radius, and θ is the polar angle. The adjustment

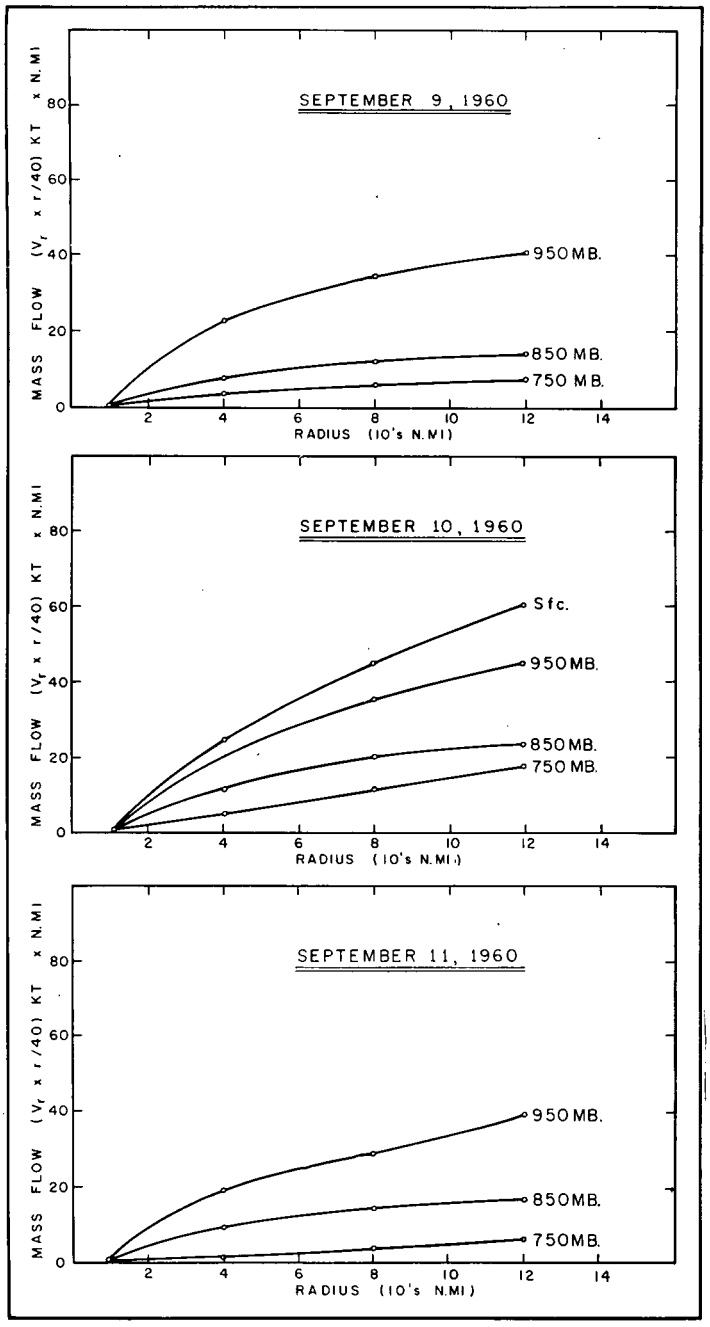

FIGURE 6.—Radial profile of mass flow ($v_r \times r$).

required to achieve mass balance was small, less than 1 kt. on each of the three days. The vertical profiles are similar to those obtained from mean data (Jordan [12]; Miller [16]) as well as those observed in several individual cyclones (e.g., Malkus and Riehl [15]; Miller [18]).

Figure 5 shows that practically all of the inflow into the cyclone took place below the 700-mb. level. This is typical of most hurricanes. The layer from the surface to 700 mb. will be referred to as the *inflow layer*. For the inflow layer it was a relatively simple matter to express the mass flow as a function of radius, although some subjectivity entered into the determination of the mass

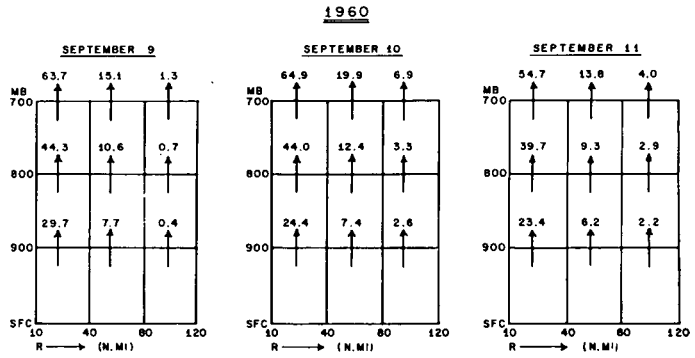

FIGURE 7.—Vertical motion (cm. sec.$^{-1}$). Data represent means for radial intervals shown.

flow for the 40-n. mi. radius. Data were tabulated at radial intervals of 40 n. mi. and at azimuthal increments of 30° in order to facilitate the subsequent energy calculations. The mean radial profiles of the mass flow are shown in figure 6. It will be noted that the mass flow changed very little during the 3-day period.

Since an accurate knowledge of the mass flow is of fundamental importance in explaining the energy processes of the tropical cyclone, it is desirable to check the accuracy of the mass flow computations as closely as possible. There are two simple ways of doing this.

From the mass flow curves, the mean vertical motion for the various radial intervals may be computed. The mean horizontal velocity divergence is

$$\overline{\text{Div } \mathbf{V}} = \frac{1}{r}\frac{\delta}{\delta r}(\bar{v}_r r) \qquad (2)$$

the overbar indicating mean values. With values of divergence from (2) the vertical motion was computed for the 900-, 800-, and 700-mb. levels. The results are shown in figure 7. Inside the 40-n. mi. radius the computed vertical velocities at the 900-mb. level range from 23 to 30 cm. sec.$^{-1}$, which is comparable to the values of 28 to 37 cm. sec.$^{-1}$ obtained inside this radius by Malkus and Riehl [14] at the 1.1-km. level for their semitheoretical model.

At the top of the inflow layer the range of vertical motion inside the 40-n. mi. radius is 55 to 65 cm. sec.$^{-1}$ If most of the ascent takes place in the form of updrafts inside undilute cumulonimbus towers which cover up to 10 percent of the inner area (as suggested by Malkus and Riehl [14]), then these updrafts must reach speeds of about 10 to 16 kt. These values are considered reasonable, and are of the order frequently encountered (based on estimates by experienced hurricane reconnaissance pilots) near the eye region of mature hurricanes. Recently, Gray [6] has made some computations of draft scale vertical motions of this magnitude near the core of several hurricanes.

An independent check on the mass flow for the 120-n. mi. radius was obtained by computing the moisture budget for the 11th. The moisture equations may be written as

$$\overline{P}=\oint\int_{p_0}^{p_t} v_r q ds \frac{dp}{g}+\int_A EdA-\delta M/\delta t \qquad (3)$$

where $\overline{P}$ is the average precipitation rate over the area A, q is the mixing ratio, E is the evaporation and, M is the total moisture content inside the volume. The vertical integration extended from the surface (p_0) up to 200 mb. (p_t) at which level the mixing ratio was small enough to be neglected. Equation (3) can be used to evaluate the mean precipitation rate for the area inside the 120-n. mi. radius. This rate can then be compared with the precipitation measurements on the 11th when the center was over land.

For the 11th, hourly rainfall measurements from a total of 45 recording rain gages were composited with respect to the center of the cyclone. Data for the period 0000–1200 GMT were plotted and then averaged over squares with sides of 40 n. mi. The mean isohyetal pattern is shown in figure 8. The rate of precipitation for the area was 181.53×10^9 gm. sec.$^{-1}$ The rate computed by use of equation (3) was 249.76×10^9 gm. sec.$^{-1}$ The ratio of observed to computed is 0.73 (table 1). This is considered excellent agreement, since rain gages (even when shielded) do not catch the total precipitation in high winds, such as those observed in hurricanes (Miller [17]). The computed precipitation rate is probably more accurate than that obtained from the rain gage network.

The mass flow described in figures 5 and 6 resulted in computed precipitation rates consistent with the measured rainfall (on one day at least), and the vertical motions implied by the mass flow curves seem reasonable. The vertical mass flow curves are not unlike those observed in other tropical cyclones. It is apparent that the mass flow has been described as accurately as any available observational data permit. These data will be used to compute the energy transformations which took place within the cyclone.

Before discussing the energy computations we shall examine briefly a few of the structural changes which occurred in the cyclone following landfall. Figure 9 shows the radial profiles of the surface pressure on the 10th and 11th. Outside the 40-n. mi. radius the data used in preparing figure 9 were obtained by averaging around the cyclone. Inside that radius individual barograms were used, time changes were converted to space changes, and symmetry of the pressure field was assumed. On the 10th the central pressure was about 929 mb.; and near the center the steep pressure profile of the intense hurricane was in evidence. By 0600 GMT on the 11th, the central pressure had risen to about 965 mb. and the slope of the pressure profile near the core had diminished. While the pressure at the center rose after landfall, the pressure outside the 40-n. mi. radius actually decreased. This represents a redistribution of the mass of the cyclone during the filling process.

The radial profiles of the low-level winds also show some significant changes. Outside the 40-n. mi. radius,

TABLE 1.—*Measured and computed precipitation rates for area of cyclone inside radius of 120 n. mi., 0000–1200 GMT, September 11, 1960*

Date	Precipitation (mm./hr.)		Ratio of observed to computed
	Observed	computed	
September 11	4.3	5.9	0.73

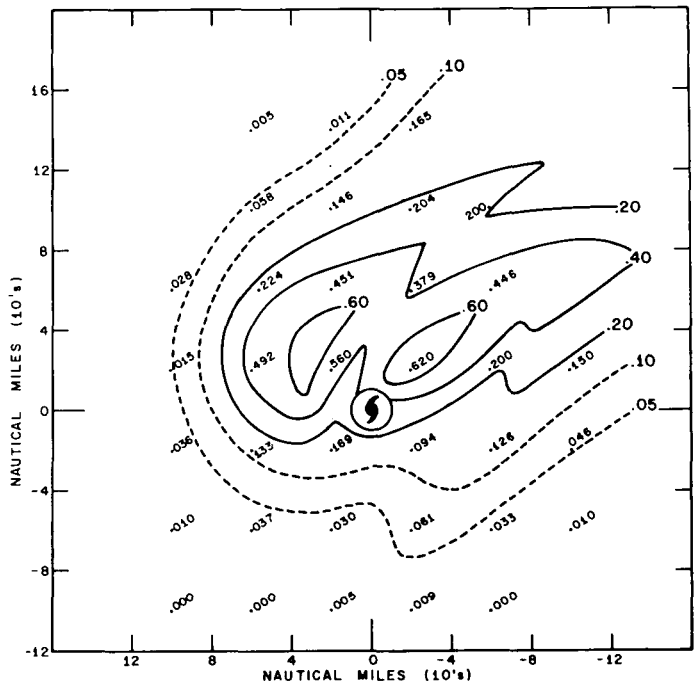

FIGURE 8.—Mean isohyetal pattern, September 11, 1960. Amounts in inches/hour.

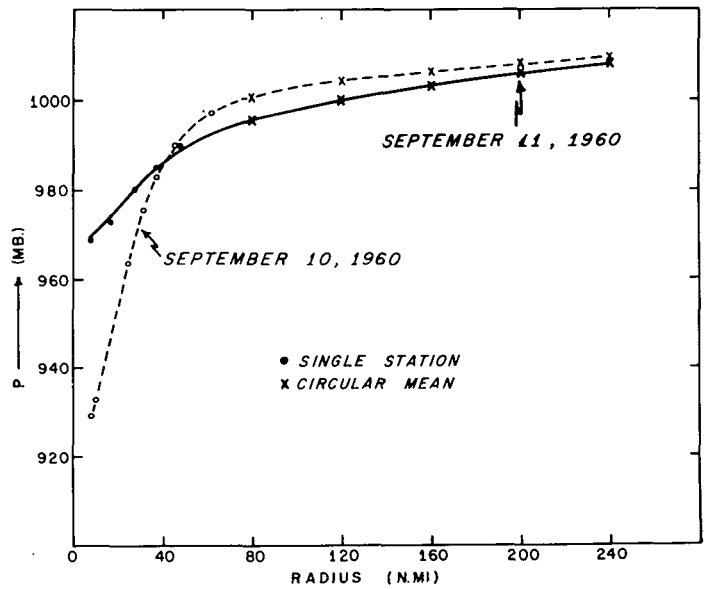

FIGURE 9.—Radial profiles of surface pressure, 0600 GMT.

wind speeds for the surface to 900-mb. layer were averaged around the cyclone and plotted on a logarithmic scale (fig. 10). On the 9th and 10th (when the center was over water) the profiles are similar. On these two days the wind profile is described reasonably well by the vortex model Vr^x=constant, with x having the values of 0.47 and 0.48. The maximum sustained wind measured over water was about 111 kt. at Sombrero Lighthouse. On the 11th the slope of the profile outside the 80-n. mi. radius did not change very much, but inside this radius $Vr^{0.32}$= constant yields the line of best fit.

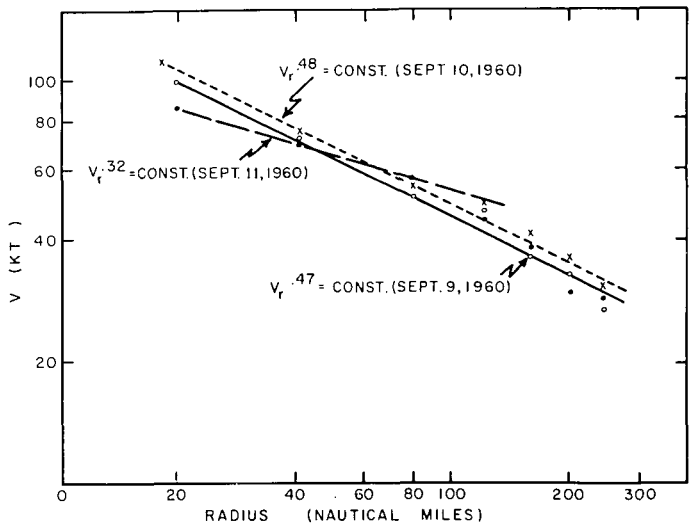

FIGURE 10.—Radial profiles of surface to 900-mb. mean layer winds.

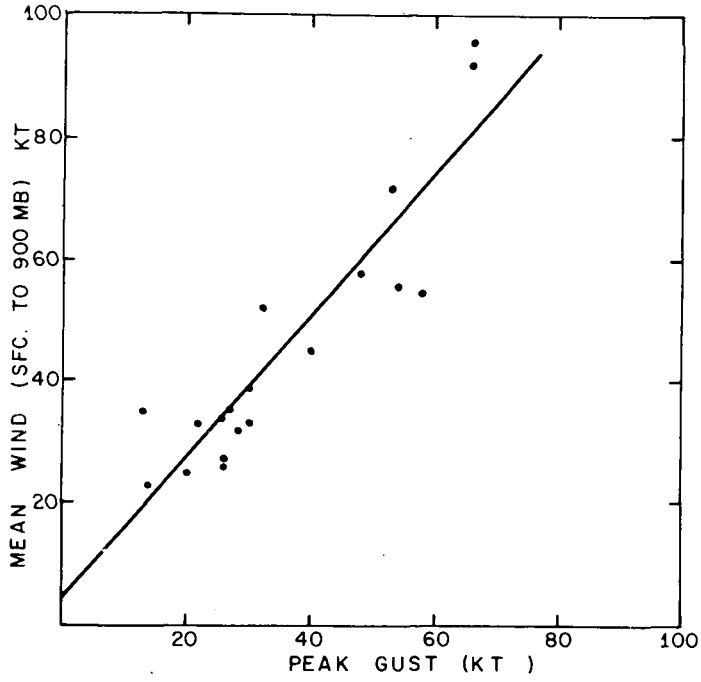

FIGURE 11.—Mean wind (surface to 900 mb.) as a function of the peak surface gust.

Inside the 40-n. mi. radius on the 9th and 10th, the profiles are based on wind reports from island or lighthouse stations and these were used to estimate the mean wind for the surface to 900-mb. layer in accordance with the well known fact that over the oceans the vertical wind shear in tropical cyclones is small. Over land, however, the vertical shear is greater than it is over water, and surface winds near the core of the cyclone could not be used to represent the mean wind for the layer extending from the surface up to 900 mb. The mean wind for this layer was plotted against the surface peak gust for rawin stations which also had gust recorders. These data are shown in figure 11. The peak gust is the highest recorded the hour when the rawin balloon was released. In general it will be noted that the mean wind is about 10 to 15 percent higher than the peak gust. The peak gust at Lakeland, Fla., when the eye was within about 8 n. mi. of the station, was 78 kt. Hence we have estimated the maximum wind (mean for the surface to 900-mb. layer) over land at 0600 GMT on the 11th as 85 kt. This value is consistent with the wind profile obtained for the outer portions of the cyclone.

3. THE FLUX OF ENERGY ACROSS THE LOWER BOUNDARY

We shall now compare the flux of energy across the air-sea interface with the flux across the air-ground interface. In any comparison of this type the problem arises as to the proper value of the exchange coefficients to be used. Since these energy exchanges at the surface may be of paramount importance to our problem, it is necessary to spend some time to obtain the best possible estimate of these exchange coefficients. The working forms of the diffusion equations to be used are

$$Q_s=\rho c_h c_p(T_s-T_a)V_0 \tag{4}$$

$$Q_e=LE=\rho L c_e(q_s-q_a)V_0 \tag{5}$$

$$\tau=\rho c_d V_0^2 \tag{6}$$

where Q_s and Q_e are the fluxes of sensible and latent heat; ρ is the density of air at the surface; c_h, c_e, and c_d are nondimensional exchange coefficients for sensible heat, latent heat, and momentum; c_p is the specific heat of air (at constant pressure); T_s is the temperature of the underlying surface, T_a is the temperature of the air; L is the latent heat of condensation; E is evaporation; q_s is the saturation mixing ratio corresponding to T_s, q_a is the actual mixing ratio; V_0 is the wind speed at anemometer level, and τ is the horizontal shearing stress.

The form and accuracy of equations (4)–(6) have been the subject of much discussion in the literature (Thornthwaite and Holzman [34]; Jacobs [11]; Sverdrup [33]; Deacon and Swinbank [3]; Sheppard [32]; Priestley [25]; Petterssen et al. [23]). Their accuracy undoubtedly leaves

much to be desired, but they have given some useful results (Jacobs [11]; Riehl et al. [27]; Malkus and Riehl [15]; Miller [18]). The main weakness in these expressions is the implied assumption that the vertical profiles of wind, temperature, and moisture are similar in shape and that the physical processes responsible for turbulent diffusion of momentum, heat, and moisture are also similar (Priestley [25]). There is no valid reason to suppose that the physical processes are similar.

Over water the roughness itself is a function of the wind speed which makes the determination of c_d somewhat difficult, as a survey of the literature will reveal. The difficulty of determining c_h and c_e is even greater. However, the success of various formulas (e.g., Thornthwaite and Holzman [34], Petterssen et al. [23]) which are based on the equality of these coefficients, lends support to the use of $c_d=c_h=c_e$ as a working rule. Deacon and Swinbank [3] measured surface stress and evaporation and then calculated evaporation, assuming that K_w (eddy diffusivity) and K_m (eddy viscosity) are equal. Their tests gave a value of $K_w/K_m=1.04\pm0.09$. Rider [26] obtained an experimental value of 1.12 ± 0.04 for the ratio. Both of these values indicate an approximate equality between K_m and K_w. Since there is definite knowledge that the magnitudes of the coefficients are of the same order, we will obtain a first approximation of the various vertical fluxes by making the simple assumption that the various coefficients are equal.

Sverdrup [33] has summarized the available computations of c_d over water. There is much scatter, but the data may indicate a sort of parabolic distribution, with c_d reaching a minimum near winds of 6 m. sec.$^{-1}$, then gradually increasing to about 3.3×10^{-3} at winds of 25 m. sec.$^{-1}$. Wilson [35] collected computations from 46 different sources and attempted to adjust all values of c_d to a standard height of 10 m. He then divided the results into "light" and "strong" winds. For strong winds the drag coefficient ranged from 1.5 to 4.0×10^{-3}, with a mean of 2.37×10^{-3} and a standard deviation of 0.56×10^{-3}. For light winds the mean was 1.49×10^{-3} and the standard deviation was 0.83×10^{-3}.

For winds of hurricane force there are almost no estimates of the drag coefficient. Palmén and Riehl [21] used composite data compiled by Jordan [12] and Hughes [10] to calculate c_d, and obtained a range of 1.1 to 2.2×10^{-3} for winds of about 6 to 26 m. sec.$^{-1}$ Miller [18] computed c_d for hurricane Helene, using aircraft data from which he prepared an angular momentum budget, and obtained values ranging from 2.4×10^{-3} to 3.2×10^{-3} (winds 30 to 40 m. sec.$^{-1}$). The latter results represent an almost linear extension of the Palmén-Riehl data.

For use in making the Donna calculations, c_d was determined by vertical integration of the tangential equation of motion from the surface to the top of the inflow layer. In a cylindrical coordinate system, with radius, r, and radial velocity, v_r, positive outward, the polar angle, θ, and the tangential velocity v_θ, positive in a cyclonic sense, the height, z, and the vertical motion, w, positive upward, the tangential equation of motion may be written

$$\frac{dv_\theta}{dt}=-\frac{1}{\rho}\frac{\partial p}{r\partial\theta}-fv_r-\frac{v_rv_\theta}{r}+\frac{1}{\rho}\frac{\partial\tau_{\theta z}}{\partial z} \tag{7}$$

in which lateral friction has been neglected. In (7) p is the pressure, f is the Coriolis parameter, and $\tau_{\theta z}$ is the shearing stress in the θ-z plane.

By assuming (1) steady state (relative to a moving coordinate system), and (2) that the tangential gradients of pressure and of v_θ are negligible, equation (7) may be written as

$$\frac{\partial\tau_{\theta z}}{\partial z}=\rho v_r\zeta_a+\rho w\frac{\partial v_\theta}{\partial z} \tag{8}$$

where ζ_a is the absolute vorticity. Assumptions (1) and (2) are probably justified in most mature tropical cyclones (Malkus and Riehl [15]; Rosenthal [30]). More serious is the neglect of lateral friction. The lateral transfer of momentum near the eye may be large. Such transfer, however, cannot be evaluated with sufficient accuracy to be included here.

Equation (8) can be integrated from the surface to the top of the inflow layer, which gives (using pressure as the vertical coordinate)

$$\tau_{\theta0}-\tau_{\theta h}=\int_{p_0}^{p_h}v_r\zeta_a\frac{dp}{g}+\int_{p_0}^{p_h}w\frac{\partial v_\theta}{\partial z}\frac{dp}{g} \tag{9}$$

At the top of the inflow layer $\bar{v}_r$ is zero and the vertical wind shear is very nearly zero (Hawkins [8]). Therefore, $\tau_{\theta h}$ should be small, and the surface stress can be approximated by the use of (9).

The second integral could not be evaluated for all days at all radii, and in computing the surface stress it had to be omitted. However, an estimate of its magnitude could be obtained on the 9th by use of aircraft data along the tracks shown in figure 2. Winds at the three levels (1600,6400, 14,200 ft.) were averaged along the closed paths and then adjusted to a common radius of 50 n. mi. These data indicated a vertical shear of -6 kt. from 1600 to 6400 ft. and -2 kt. from 6400 to 14,200 ft. Using this vertical profile and the vertical motion from figure 7, the second integral of (9) was evaluated and found to be less than 10 percent of the first integral. This is in agreement with an estimate by Rosenthal [30], since near the surface where vertical wind shear is large the vertical motion is negligible, and near the top of the inflow layer where the vertical motion is large the vertical shear is negligible. This is almost certainly true for mean profiles. If most of the vertical ascent takes place within a few large cumulonimbus clouds, the integration of (9) becomes more difficult. In any event the second integral probably represents only a small correction to the results obtained by evaluation of the first integral. Consequently, the surface stress was estimated from the first integral of (9).

TABLE 2.—*Surface stresses and drag coefficients computed by integration of tangential equation of motion through inflow layer, Hurricane Donna, September 1960.*

Date	Radius (n. mi.)	Surface stress (dynes/cm²)	Surface wind V_0 (m./sec.)	Drag coefficient c_d (×10³)
September 9	40	54.00	36.0	3.60
9	80	23.16	27.8	2.61
9	120	11.88	25.2	1.63
9	160	6.39	19.0	1.54
9	200	5.56	17.3	1.62
10	20	130.04	52.0	4.19
10	30	89.04	43.8	4.03
10	40	59.74	38.0	3.60
10	80	30.56	28.3	3.33
10	120	19.25	25.2	2.64
11	40	62.72	24.2	8.73
11	80	34.75	20.0	7.37
11	120	11.76	17.0	3.54

Calculations of the surface stresses were made for each of the three days at several radii. The drag coefficient was then determined by the use of (6). The results are shown in table 2.

The coefficients in table 2 represent means since both v_r and ζ_a were averaged around the cyclone as well as vertically. On the 9th and 10th the cyclone center was over water and the results should be comparable to the Palmén-Riehl and Helene calculations, although at radii greater than 80 n. mi. portions of the cyclone were over land on both days. (The percentage of the total area over land is shown in table 4.) The greater roughness over land undoubtedly has some influence on the results shown in table 2. Figure 12 shows a plot of c_d as a function of the wind speed over water; the Palmén-Riehl and the Helene calculations have been added to the Donna data for the 9th and 10th. It is clear that there is reasonable agreement between the Donna calculations and earlier results. These values will be used in computing the energy fluxes by means of equations (4)–(6).

Before doing so, however, we must estimate the quantities $(T_s - T_a)$ and $(q_s - q_a)$. Since there were not many ship reports inside the 120-n. mi. radius, this required some extrapolation of the available data. Water temperatures were composited for a 2-day period (September 7–8) in order to obtain some estimate of the sea surface temperatures prevailing within the area prior to the passage of the cyclone. These data were averaged by 5° squares. The average water temperature in the area over which Donna was to pass on the 9–11th was about 29.0° to 29.5° C., which is near or slightly above the climatological average for September. The water temperatures for the 9th, 10th, and 11th were also composited (four 6-hourly map times on each chart). There was some slight indication of a drop in water temperature after the passage of the cyclone. This cooling of the water after the passage of the cyclone is not unexpected and has been observed before (Fisher [5]; Pike [24]). It is probably due to a combination of (1) removal of sensible heat by the cyclone, (2) upwelling, (3) mixing with several inches of rain water, which is somewhat colder than the sea

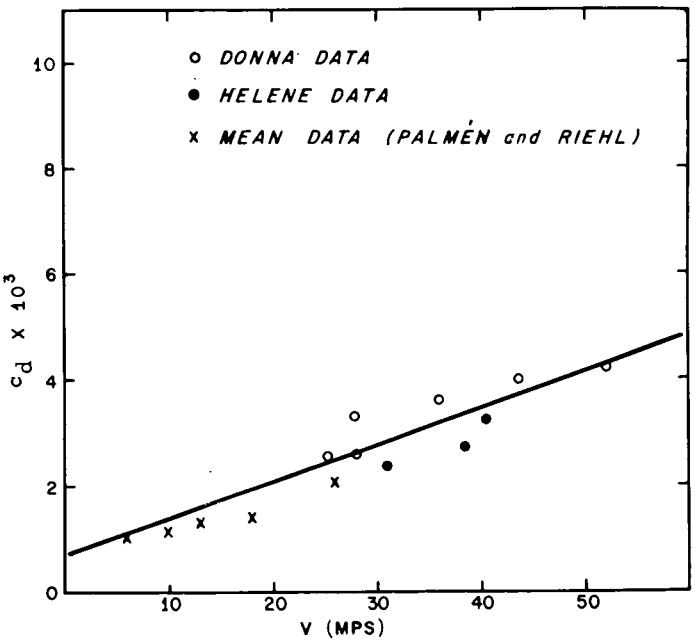

FIGURE 12.—Drag coefficient (c_d) as a function of wind speed over water.

surface water, (4) reduction of insolation by heavy clouds, and (5) mixing within the ocean.

The available data are not good enough to permit an exact determination of the average sea surface temperature inside the area of interest. The data do suggest a gradual transition from about 29.0° C. in the forward half of the cyclone to near 27.0° in the rear. These values were used to compute the heat fluxes on the 9th and 10th. On the 11th the rear of the cyclone was over land, and since the only significant heat flux occurred in the front half, an average of 29.0° C. was used.

Temperatures and dew points of the surface air were plotted for the three compositing periods (0000–1200 GMT) on the 9th, 10th, and 11th. The data for the 10th and 11th are shown in figures 13 and 14. Over water the average surface temperature within the 40–120-n. mi. area was about 26.0°C., while the average of ten dropsonde observations in or near the eye between the hours of 0000 GMT and 1310 GMT on the 9th and 10th was 27.0°C. The corresponding average dew point temperature was 25.8°C. These data are consistent with an estimate of a surface air temperature of 26.0°C. in the wall cloud region on the 9th and 10th. This value was used, and gives an average air-sea temperature difference of 3.0°C. in the forward and 1.0°C. in the rear half. The areal average was 2.0°C., which is in agreement with estimates for other cyclones in the Atlantic area (Malkus and Riehl [15]; Miller [18]). The average dew point at the 120-n. mi. radius was about 24.0°C. on the 9th and 10th; this increased to about 25.8°C. in or near the eye. Figure 14 shows that the surface temperatures and dew points near the eye over land were about 2°–3°C. lower than they were over water.

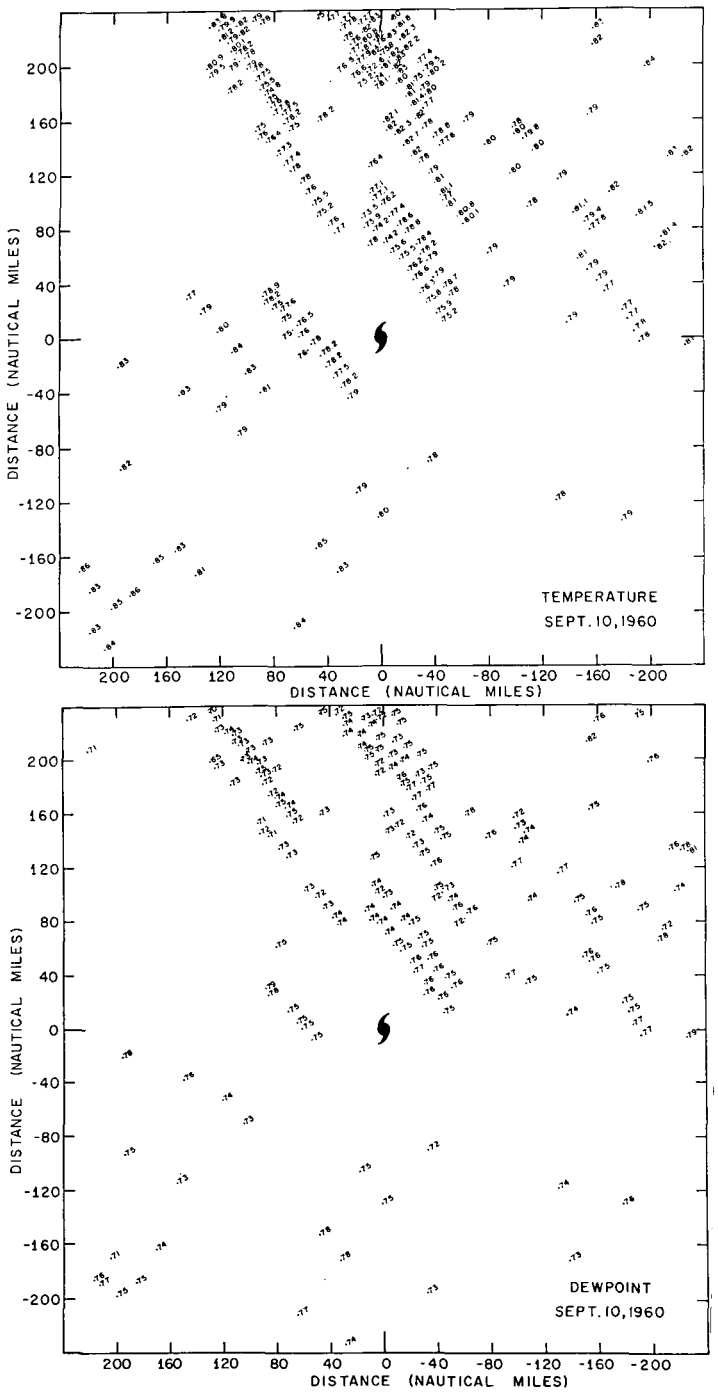

FIGURE 13.—Temperatures and dew points of the surface air on September 10, 1960.

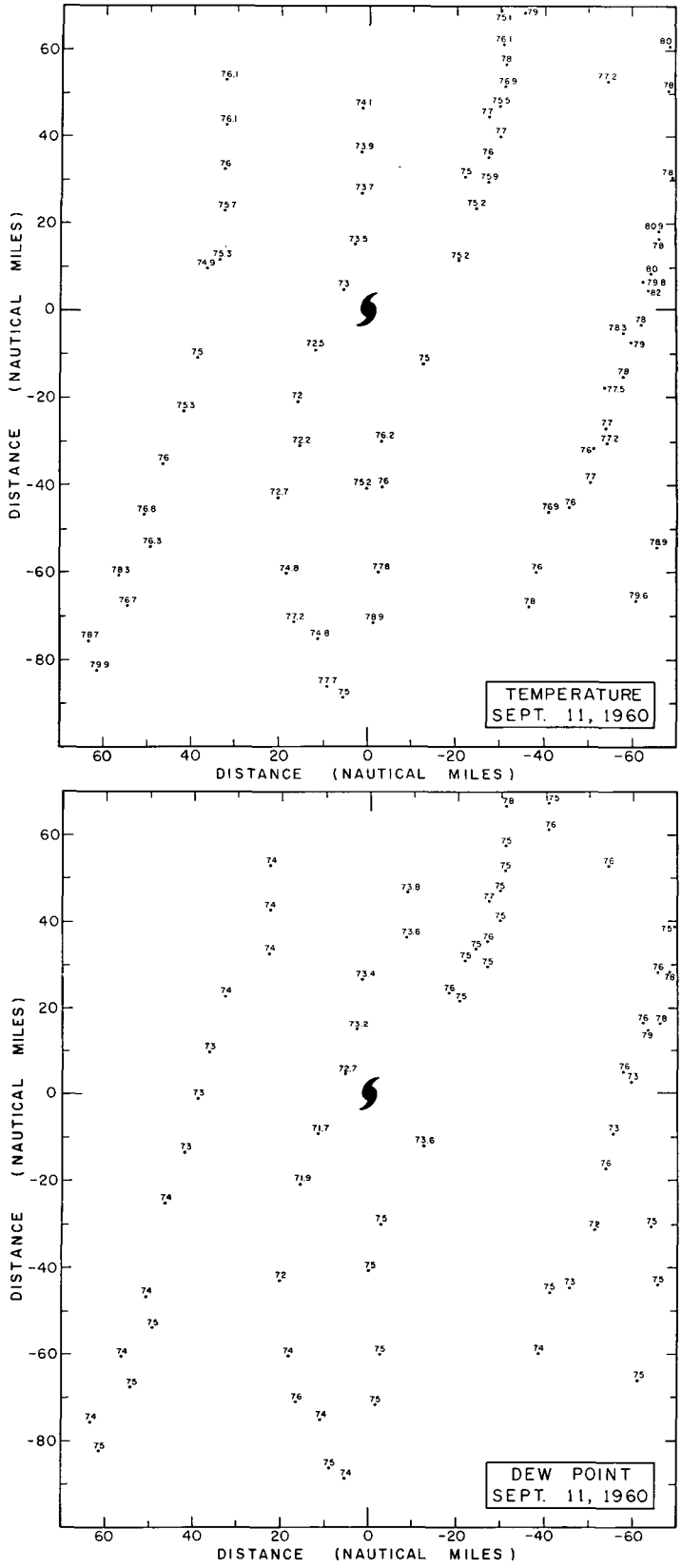

FIGURE 14.—Temperatures and dew points of the surface air on September 11, 1960.

The presence or absence of a surface heat source may be determined by calculating the sensible and latent heat transfers along a trajectory as the surface air flows inward toward the core of the cyclone. The sensible heat transfer may be obtained by integration of the equation which expresses the first law of thermodynamics along a trajectory. This gives

$$\Delta Q_{sp}=c_p(T_2-T_1)+R\bar{T}\ln p_1/p_2 \qquad (10)$$

where ΔQ_{sp} (cal./gm.) is the change in sensible heat content along a trajectory. T is the temperature, R is the gas constant, and p is the pressure.

Similarly,

$$\Delta Q_{ep}=L(q_2-q_1) \qquad (11)$$

in which ΔQ_{ep} (cal./gm.) is the gain or loss in latent heat following the motion of a parcel, q is the mixing ratio, and L is the latent heat of condensation.

Four trajectories were constructed from composited surface data for the 10th. These are shown in figure 15. These are *relative* trajectories. The wind data are from lighthouse stations, supplemented by coastal stations along the Florida Keys. The trajectories were computed by *working backwards;* i.e., from a selected point near the core of the cyclone (where temperatures, pressures, and dew points were known from dropsonde data) the parcel was traced back until a place was reached for which initial values of temperature, pressure, and dew points were known. Seven trajectories were constructed for the 11th. These are shown in figure 16. These were constructed from streamline-isotach analyses of hourly charts, using the method described by Petterssen [22]. These were also constructed by working backward. For both days there is probably some error in locating the exact origin of the air which eventually reached the core of the cyclone at the center. However, this is not important, since the peripheral surface air near the

TABLE 3.—*Latent and sensible heat transfer (Q_{ep} and Q_{sp}) in cal./gm. following the motion of a particle at the surface*

Trajectory Number	Radial Interval (n. mi.)	Length of Trajectory (n. mi.)	Q_{sp} cal./gm.	Q_{ep} cal./gm.
Over-Water Trajectory				
1	24–66	75	1.22	1.98
2	20–65	60	1.09	1.60
3	20–65	140	.93	1.92
4	12–57	75	1.43	2.37
Average			1.17	1.97
Over-Land Trajectory				
1	32–96	95	0.41	−0.29
2	20–80	60	0.51	0.41
3	36–90	76	−0.27	−0.04
4	26–78	96	−0.20	−1.17
5	20–80	80	−0.13	−0.73
6	7–80	84	−0.17	−0.91
7	36–74	70	−0.04	−0.20
Average			0.01	−0.36

739–756—64——3

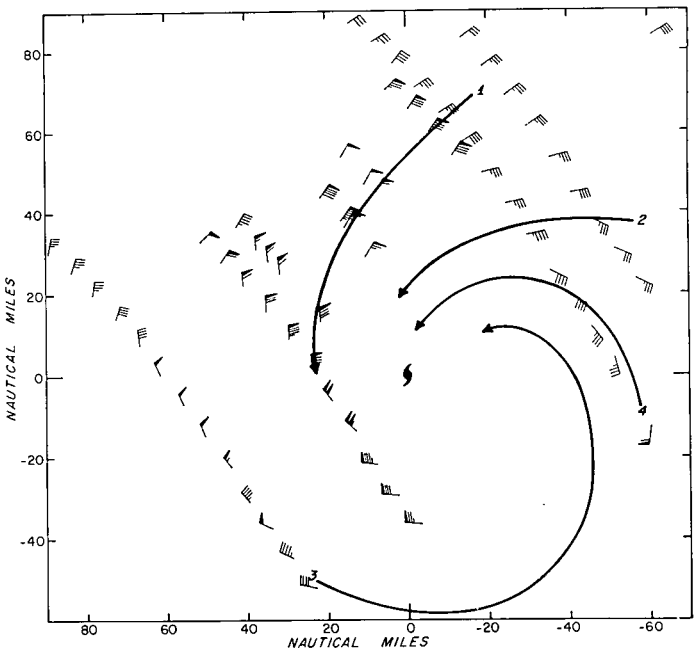

FIGURE 15.—Surface trajectories over water. These are relative trajectories.

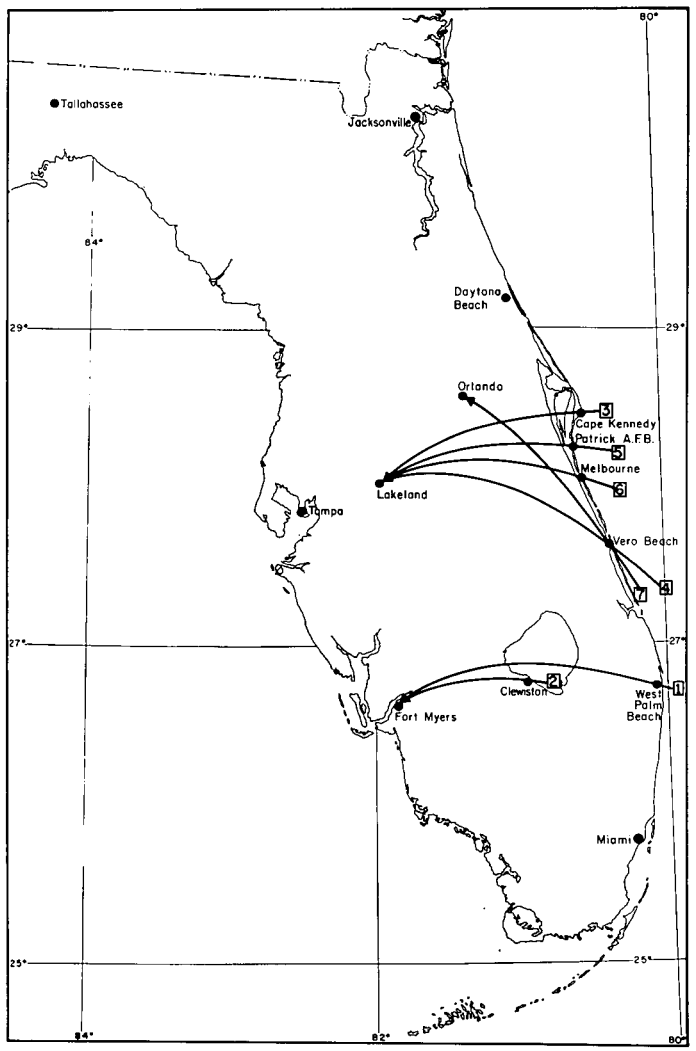

FIGURE 16.—Surface trajectories over land.

TABLE 4.—*Surface energy sources and sinks for 3-day period*

Date	9	9	9	9	10	10	10	10	11	11	11	11
Radial Interval (n. mi.)	10–40	40–80	80–120	10–120	10–40	40–80	80–120	10–120	10–40	40–80	80–120	10–120
V_0 (m. sec^{-1})	42.0	30.0	24.0		45.0	32.0	25.0		28.5	22.0	18.5	
(T_s-T_a) (°C.)	2.0	2.0	2.0	2.0	2.0	2.0	2.0	2.0	0.0	†3.0	†3.0	†3.0
$c_d\times10^3$	3.90	3.05	2.10		4.00	3.40	2.90		*8.70	*8.25	*5.50	
										#2.40	#2.00	
Percentage of area over land	0	15	30	21	0	16	29	21	100	65	33	50
$Q_s\times10^{-12}$ (cal./sec.)	1.46	2.21	1.68	5.35	1.61	2.60	2.47	6.68	0	.78	1.75	2.53
(q_s-q_a) (gm./kg.)	3.08	3.55	4.36		3.08	3.55	4.36			5.30	6.50	
$Q_e\times10^{-12}$ (cal./sec.)	5.47	9.57	8.84	23.88	6.03	11.25	13.04	30.32	0	3.33	9.34	12.67
Bowen ratio	.27	.23	.19	.22	.27	.23	.19	.22		.23	.19	.20
Ground friction ($\times10^{-12}$ cal./sec.)	1.43	1.42	.80	3.65	1.48	1.64	1.15	4.27	.89	1.34	.84	3.07

*mean c_d over area used in computing ground friction.
#mean c_d for portion of area over water used in computing Q_s and Q_e.
†for portion of cyclone over water.

origin of the trajectories was relatively homogeneous (figs. 13 and 14). The intent here is to show the different sensible and latent heat contents between the center and the periphery on the two days. The results are summarized in table 3.

Over water the increase in both sensible and latent heat along the trajectories was very large, as expected. The equivalent potential temperatures increased rapidly as the core was approached. Over land only two of the seven trajectories show any appreciable increase in sensible heat. These two passed over the Everglades in southern Florida, a low-lying and swampy area, and some vertical heat flux is not unexpected. The other five trajectories show a decrease in sensible heat, such that the average is very nearly zero. There was some net loss (on the average) in latent heat content, since some condensation took place along the trajectories. These calculations show that surface inflow over land is essentially a *moist adiabatic process*. This effectually demonstrates that following landfall the tropical cyclone was removed from its surface heat source.

It is now possible to compare the flux of energy through the lower boundary of the cyclone for the 3-day period. Heat fluxes may be obtained by integrating equations (4) and (5) over the areas. The surface frictional dissipation of kinetic energy may be determined by forming the scalar product of $\mathbf{V}\cdot\tau$ and then integrating over the area (Malkus and Riehl [14]). This gives

$$F_s=\int_A \rho c_d V_0^3 dA \qquad (12)$$

The results of the calculations of the energy exchange at the surface are summarized in table 4. Table 3 indicated that the fluxes of latent and sensible heat over land are very nearly zero, and zero fluxes have been shown for all land areas.

On the 9th and 10th the vertical fluxes of both sensible and latent heat were larger than had been found to exist in either Daisy (Malkus and Riehl [15]) or Helene (Miller [18]). Inside the 80-n. mi. radius on the 10th the average sensible heat flux was 0.62×10^{-2} cal. cm.$^{-2}$ sec.$^{-1}$, or 535 cal. cm.$^{-2}$ day^{-1}, and the average latent heat flux was (in the same units) 2.86, or 2471. Average values found in Daisy inside the 80-n. mi. radius on the day of maximum intensity were 250 cal. cm.$^{-2}$ day^{-1} for the sensible heat flux, and 1425 cal. cm.$^{-2}$ day^{-1} for the latent heat flux. The Donna values are comparable to the oceanic heat source predicted by Malkus and Riehl [14] for their semi-theoretical model. For the area lying between radii of 30 and 90 km., with maximum winds of 112 kt., they obtained values (in cal. cm.$^{-2}$ day^{-1}) of 720 for sensible heat flux and 2420 for latent heat flux. The agreement is striking, particularly when one recalls that the maximum sustained winds in Donna were about 111 kt.

On the 11th the surface heat source inside the 40-n. mi. radius was cut off, although there was still some vertical heat flux from the ocean outside this area, since at 0600 GMT 35 percent of the area between the 40 and 80-n. mi. radii was still over water. However, it is the heat source near the core which makes the most important contribution to the growth of the energy of the cyclone. It is within this small area that the surface heat source results in a strong radial gradient of equivalent potential temperature. It is the ascent of this surface air with greatly increased values of equivalent potential temperature that produces the warm core of the tropical cyclone. Since the release of latent heat in the absence of a radial gradient of equivalent potential temperature will not produce a warm core, the importance of the surface heat source is evident.

Table 4 shows that the frictional dissipation of kinetic energy at the surface was less over land than it was over water. This may be somewhat misleading, since the wind data used in computing surface friction were centered around 0600 GMT on the 11th, which was several hours after the center moved onshore. It appears likely that during the first few hours after landfall, frictional dissipation over land must have exceeded that over water. If this was the case, the region where this was true may have been restricted to the region near the core where the winds were *onshore*.

The maximum sustained surface wind recorded over water was about 111 kt., and the highest value computed for c_d was about 4.2×10^{-3}. Over land the maximum value for c_d was 8.7×10^{-3}. In order for the frictional dissipation over land to equal the maximum over water,

a surface wind of 86 kt. would be required. At no time were there any *sustained* surface winds of this magnitude recorded, although without a dense network of recording anemometers, it cannot be established that no such winds occurred.

The eye passed over Ft. Myers about 1930 GMT on the 10th. At this time the minimum pressure recorded at the Weather Bureau was 951 mb. (A privately owned barometer reported a minimum of 940 mb.) The maximum wind was about 80 kt. from the northeast, which would indicate less frictional dissipation over land near the core than over water just before the eye moved inland. Along the immediate coast, in the region of onshore winds, it is probable that the surface winds exceeded 86 kt. and that the dissipation due to surface friction over a small area was greater than it had been over water. Turbulence theory would suggest that there should be greater vertical shear over land than over water because of the greater roughness of the land surface. The wind slows down more at anemometer level than it does at some higher elevation. The peak gust-mean wind data (fig. 11) would indicate that this was so. This would contribute to a lessening of the surface frictional dissipation over land. The decrease in the pressure gradient over land (fig. 9) should also result in reduced frictional dissipation, by permitting the winds to decrease because of reduced pressure forces.

4. CHANGES IN THE THERMAL STRUCTURE

Next we shall examine the changes in the thermal structure in the light of the surface exchange processes and then attempt to formulate some estimate of how these thermal changes resulted in dynamical changes in the cyclone. The surface pressures are known with a high degree of accuracy, particularly on the 10th and 11th. It was also possible to prepare good analyses of the 100-mb. level (at least for the area outside the 80-n. mi. radius) for these two days. From these two levels mean virtual temperatures for the surface to 100-mb. layer were computed from

$$Z_t=\frac{RT^*}{g}\ln p_0/p_t \qquad (13)$$

where Z_t is the thickness between the two layers and T^* is the mean virtual temperature. The results are shown in figure 17.

During the 24-hr. period covered by the data of figure 17, the central pressure rose about 36 mb., but the pressure outside a radius of 40-n. mi. fell slightly. These two facts are revealed by the indicated cooling of about 3.0° C. in the center of the cyclone and a warming of about 0.6° C. outside the 40-n. mi. radius. This probably reflects a spreading out of the warm air previously concentrated near the core and a redistribution of the mass of the cyclone during the filling process.

The analysis of the 100-mb. level is a critical point here.

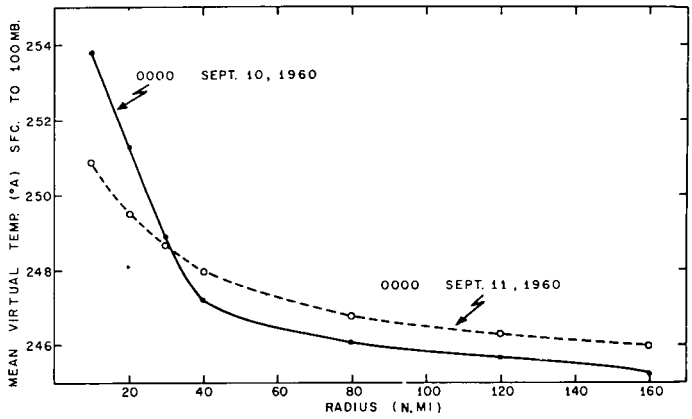

FIGURE 17.—Mean virtual temperatures (surface to 100 mb.), September 10–11, 1960. Time is GMT.

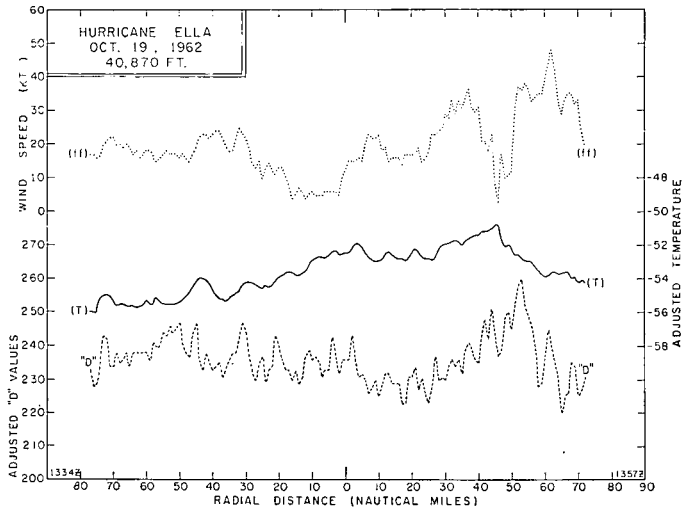

FIGURE 18.—Radial profiles of "D" value, temperature, and wind speed, hurricane Ella, October 19, 1962, at 40,870 ft.

There were very few data at this level inside the 80-n. mi. radius. It was possible to show that the 100-mb. surface was almost flat outside this radius, but it cannot be definitely established that this surface was flat nearer the core. Data from other cyclones, however, can be cited to show that where data are available some level can be found at which the constant pressure surface is relatively flat. For our argument it does not matter whether this level is at 200 mb. or at 80 mb. Figure 18 shows data collected by a flight through the center of hurricane Ella, October 19, 1962, at a level of about 41,000 ft. At that time the central surface pressure was about 962 mb.

However, the "D" value profile (deviations of the height of a constant pressure surface from the equivalent height of a standard atmosphere) indicates a very nearly level surface. Variations in temperature and wind speed were also minor. Figure 19 shows the height of the 100-mb. surface at Miami during the passage of Donna, plotted

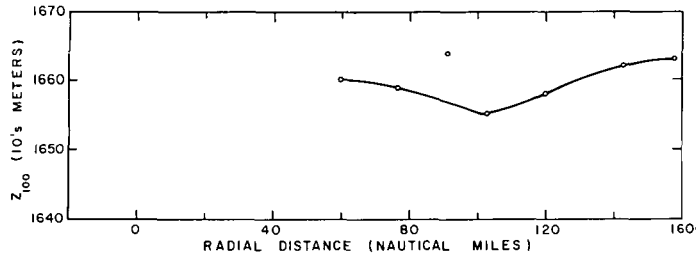

FIGURE 19.—Height of the 100-mb. surface at Miami, September 10, 1960. Radial distance is the distance of the sounding balloon from the center of the hurricane.

as a function of the distance of the sounding balloon from the center of the cyclone. The surface is virtually flat to within 60-n. mi. of the center. The heights, however, are somewhat above normal. This is in agreement with a conclusion by Rosenthal [31], based on the results of a numerical experiment, that the height of the 100-mb. surface probably rises during the development of an intense surface cyclone. It is also consistent with earlier models (Palmén [19]; Riehl [28]). We have, therefore, assumed that the 100-mb. surface over Donna was relatively flat. Until observational data can be obtained to prove that this is the case over most tropical cyclones, conclusions based on the assumed flatness of this surface must be considered as tentative.

We may choose p_0 in (13) as the surface pressure and p_t as 100 mb. Z_t then becomes the height of the 100-mb. surface. Now differentiate (13) with respect to r and t

$$\frac{\partial p_0}{\partial r,t}=\frac{p_0}{T^*}\left[\frac{g}{R}\frac{\partial Z_{100}}{\partial r,t}-\ln\frac{p_0}{100}\frac{\partial T^*}{\partial r,t}\right] \tag{14}$$

If the height of the 100-mb. surface is constant, surface pressure gradients or local changes depend primarily upon the gradient or local changes in the mean virtual temperature. To explain the surface pressure gradient, one must explain the tropospheric temperature field. This temperature field is partly dependent upon the surface heat source.

Time changes of the temperature, mixing ratio, potential temperature, and equivalent potential temperature of the surface air near the eye were prepared (fig. 20). These data are based on surface reports in or near the eye. They are intended to represent the best available estimate of surface conditions in the wall cloud region. The point for the 8th is based on a report from Ragged Island Key. The last temperature and humidity data were recorded when the eye was about 40 n. mi. from the station, but barometric pressures were recorded throughout the passage of the center. Computations were based on the assumptions of isothermal expansion, which is well documented by observational data in other cyclones (Deppermann [4]), and a relative humidity of 95 percent inside this radius. The data points for the 9th and 10th are each based on the average of five dropsonde observations made in or near the eye between the hours of 0000 GMT and 1310 GMT on each day. Other data are from land station reports; they were recorded at the time of the minimum pressure. All land station data used were within 7 mi. or less of the eye at the time of the lowest pressure.

Note first the change in the observed surface temperature. The eye began to move inland between 1200 and 1500 GMT on the 10th and 0300 GMT on the 11th. The surface air remained near saturation throughout; consequently, the reduction in temperature was associated with a sharp drop in the mixing ratio. The potential temperature also dropped, but by far the most spectacular change was in the equivalent potential temperature, which fell from a maximum of 374°A. to a minimum of 353°A.

The potential temperature and the equivalent potential temperature observed near the eye over land are characteristic of their values outside the 60-n. mi. radius while the cyclone was over the water. The temperature and mixing ratio are somewhat less as a result of moist adiabatic expansion.

The vertical temperature profiles which would result from moist adiabatic ascent of surface air having equivalent potential temperatures of 374°A. and 353°A. are plotted in figure 21. These are characteristic values of θ_e for the intense cyclone over water and the weakening cyclone over land. These curves represent the maximum values of the temperature which can occur at the upper levels; i.e., the value of θ_e at the surface limits the amount of warming within the middle and upper troposphere. At 500 mb. the temperature difference between curves "A" and "B" is about 6°C. and at 200 mb. it is about 12°C.

The processes by which the core of a tropical cyclone warms or cools may be determined from the first law of thermodynamics for moist air

$$\frac{dH}{dt}-L\frac{dq_s}{dt}=c_p\frac{dT}{dt}-\alpha\frac{dp}{dt} \tag{15}$$

where H is sensible heat per unit mass and α is specific volume. By making use of the approximation, $q_s=\epsilon e_s/p$, (ϵ being the ratio of the molecular weight of water to that of dry air, q_s and e_s the saturation mixing ratio and vapor pressure), and then introducing the Clausius-Clapeyron equation to eliminate de_s/dT (Rosenthal [30]), we obtain

$$\frac{dH}{dt}=\left[c_p+\frac{L^2\epsilon^2 e_s}{RT^2p}\right]\frac{dT}{dt}-\left[1+\frac{\epsilon e_s L}{RT_p}\right]\alpha\frac{dp}{dt} \tag{16}$$

If we now introduce an approximate form for the moist adiabatic lapse rate, dT/dp, (Haurwitz [7]), expand dT/dt, replace $\partial T/\partial p$ by Γ, $dP/dt=\omega$ (the vertical motion), and then define

$$B\equiv\left[c_p+\frac{L^2\epsilon^2 e_s}{RT^2p}\right]$$

the first law of thermodynamics for moist air (in a relative coordinate system) may be written as

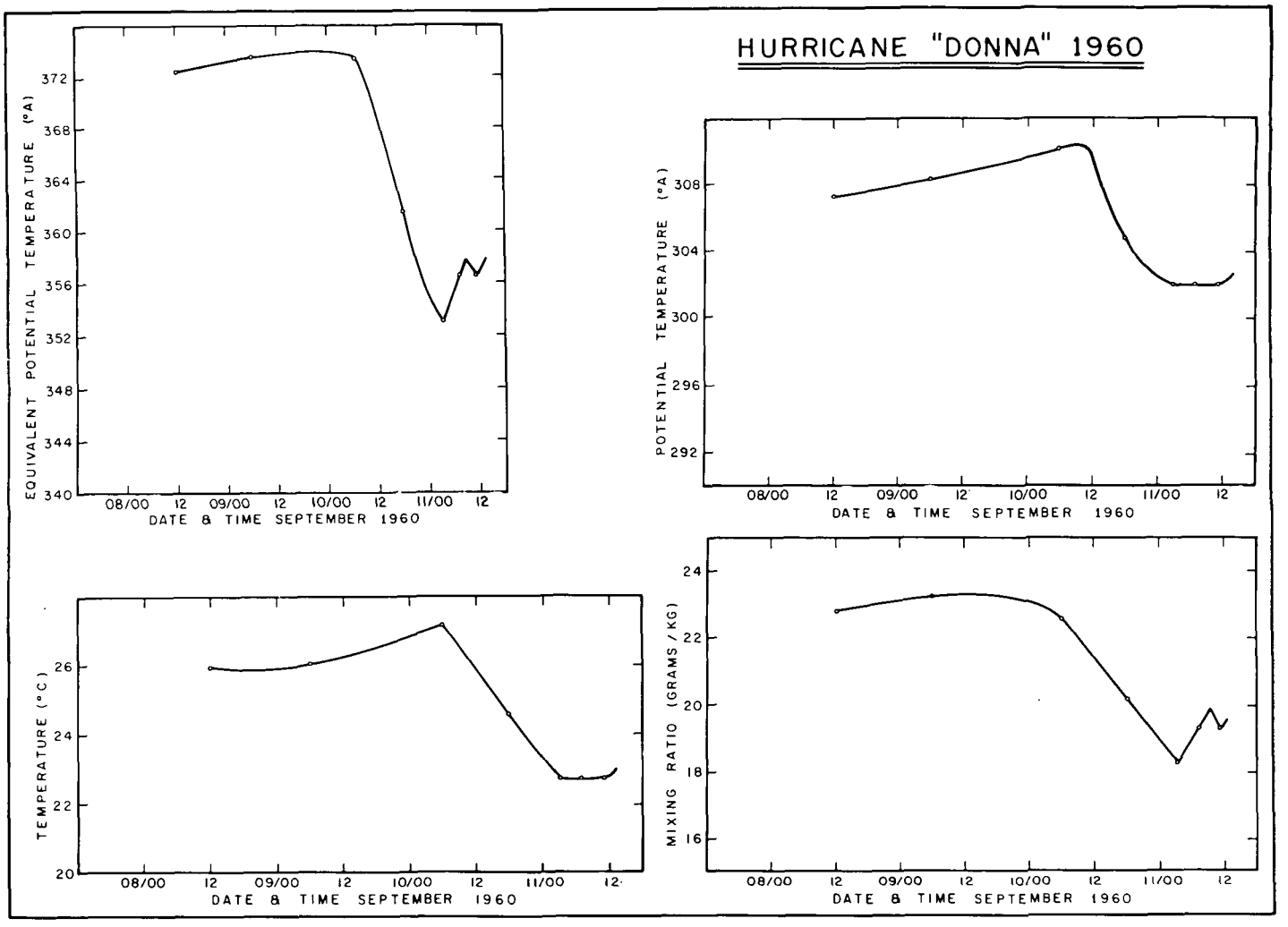

FIGURE 20.—Changes in temperature, mixing ratio, potential temperature at the surface near the eye, September 8–11, 1960. Time is GMT.

$$\frac{\delta T}{\delta t}=-\mathbf{V}_R\cdot\nabla T+\omega(\Gamma_s-\Gamma)+\frac{1}{B}\frac{\delta H}{\delta t} \qquad (17)$$

$\mathbf{V}_R$ being the relative wind.

If (17) is multiplied by $d(\ln p)$ and then integrated between two fixed pressure surfaces, p_0 and p, one obtains (after rearranging) the thickness tendency

$$\frac{\delta Z_t}{\delta t}=\frac{R}{g}\left[-\overline{\mathbf{V}_R\cdot\nabla T}+\overline{\omega(\Gamma_s-\Gamma)}+\frac{1}{B}\frac{\overline{\delta H}}{\delta t}\right]\ln p_0/p \qquad (18)$$

where the overbar indicates vertical integration. Since the tropical cyclone has a warm core, its growth and dissipation are determined by warming or cooling of the core. Equation (18) describes explicitly three thermal processes by which the cyclone intensifies or weakens: (1) lateral advection of warm or cold air into the core; (2) free convection, or the forced ascent of stable air; (3) gain or loss of sensible heat (by turbulent transfer across the lower boundary or by radiation). The first always acts to cool the core, even during the intensification process. Over

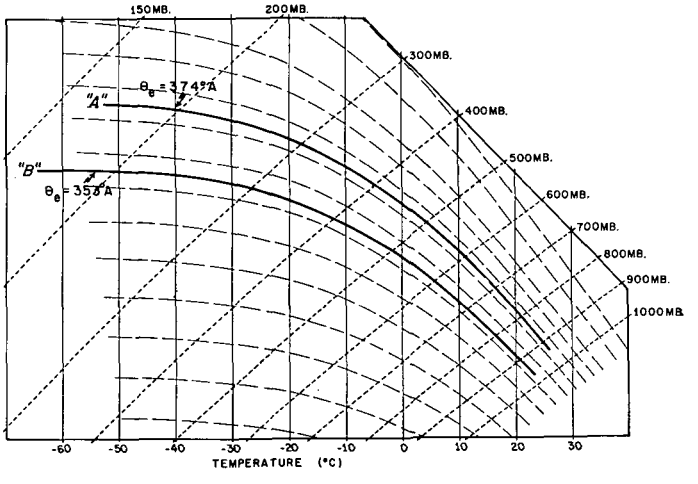

FIGURE 21.—Vertical temperature profiles following vertical ascent of undiluted surface air having equivalent potential temperatures of 353°A. and 374°A.

land the third is negligible except for the loss of heat by radiation from the tops of clouds. Hence, we must conclude that the core cools over land as a result of the forced ascent of stable air. During development the surface heat source produces the low-level instability needed to make $(\Gamma_s-\Gamma)<0$ so that ascending motion near the center results in the production of the warm core. Thus, the importance of the oceanic heat source is demonstrated in another way.

5. THE KINETIC ENERGY BALANCE

It has been shown that numerous structural, thermal, and dynamical changes occurred in the cyclone after the center moved inland. Some of these changes have been related to the removal of the oceanic heat source. It is now possible to examine the influence of these changes on the kinetic energy balance of the cyclone.

The kinetic energy equation is

$$\frac{\partial}{\partial t}\int_\alpha \rho K d\alpha = -\int_L\int_{p_t}^{p_0} v_r K dL\frac{dp}{g}-\int_A \rho\omega K dA - \int_{p_t}^{p_0}\int_A \mathbf{V}\cdot\nabla z dA dp+\int_\alpha \rho\mathbf{V}\cdot\mathbf{F}d\alpha \quad (19)$$

The first two terms on the right represent the change in kinetic energy inside the volume, α, due to transport through the boundary. The third integral is the sum of the production of kinetic energy inside the volume by pressure forces and the work done by pressure forces acting on the boundary. The last integral on the right is the frictional dissipation. The "production" term will be evaluated by the approximation

$$\int_{p_t}^{p_0}\int_A \mathbf{V}\cdot\nabla z dA dp \approx \int_{p_t}^{p_0}\int_A v_r\frac{\partial z}{\partial r}dA dp \quad (20)$$

since the height field was almost circular. The frictional dissipation term can be transformed to (Riehl [29])

$$\int_\alpha \rho\mathbf{V}\cdot\mathbf{F}d\alpha=\int_\alpha \mathbf{V}\cdot\frac{\partial\tau}{\partial z}d\alpha=\int_\alpha\frac{\partial(\mathbf{V}\cdot\tau)}{\partial z}d\alpha-\int_\alpha \tau\frac{\partial\mathbf{V}}{\partial z}d\alpha$$

The first integral on the right gives the dissipation at the upper and lower boundaries, the second, internal dissipation. We assume that the frictional stress is negligible at the top of the cyclone. Hence

$$\int_\alpha\frac{\partial(\mathbf{V}\cdot\tau)}{\partial z}d\alpha=\int_A \mathbf{V}\cdot\tau dA=-\int_A \rho c_d v_0^3 dA \quad (21)$$

Internal friction may be large (Malkus and Riehl [15]; Miller [18]), but it cannot be evaluated from the data. However, it is not necessary for our present argument.

For the inflow layer the data permitted a detailed calculation of the kinetic energy budget. This is fortunate, since the inflow layer is in essence the dynamo which runs the cyclone. The results of these calculations are summarized in table 5. The table shows the production of kinetic energy, horizontal divergence, dissipation by surface friction, and vertical transport through the upper boundary (700 mb.). The local change $(\delta K/\delta t)$ was derived from a time rate of change curve, which was prepared from the analyses of the isotach patterns.

The production of kinetic energy decreased sharply after the center moved inland. Production for the 10–120-n. mi. ring was 23.36×10^{14} kj./day on the 10th. On the 11th, when the cyclone was over land, this had decreased to 12.24×10^{14} kj./day. Within the innermost ring (10–40 n. mi.) the decrease was even more remarkable, with production dropping from 9.49 units to 3.34 units.

On the 9th, the cyclone was still intensifying, and the inflow layer produced some excess kinetic energy which may either have been exported by small-scale eddy stresses (either vertically or horizontally) or dissipated by internal friction. On the 10th there was a large amount left over for either export or internal friction. At this time the cyclone was in steady state. It is postulated that the excess was exported vertically by means of strong updrafts in cumulonimbus clouds, and later that it was either exported horizontally by the mass outflow in the upper troposphere or dissipated by doing work in the region where the outflow was against the pressure gradient. On the 11th the inflow did not produce enough kinetic energy to overcome surface friction and to provide that exported vertically by the mass circulation. None was left over for internal friction. Consequently, the

TABLE 5.—*Kinetic energy budget for the inflow layer (surface to 700 mb). Units are 10^{14} kj./day. Negative values indicate production and inward transport. $\delta K/\delta T$ is the local change of kinetic energy in a moving coordinate system*

Date	9	9	9	9	10	10	10	10	11	11	11	11
Radial Interval (n. mi.)	10–40	40–80	80–120	10–120	10–40	10–80	80–120	10–120	10–40	40–80	80–120	10–120
Production	−8.09	−4.71	−4.32	−17.12	−9.49	−7.97	−5.90	−23.36	−3.34	−5.10	−3.80	−12.24
Lateral Divergence	−4.63	−0.58	−0.08	−5.29	−5 37	−1.34	−1.89	−8.60	−4.76	−0.40	0.38	−4.78
$c_d\times10^3$	3.90	3.05	2.10	----------	4 00	3.40	2.90	----------	8.70	8.25	5.50	----------
Dissipated by surface friction	5.18	5.15	2.88	13.21	5.37	5.92	4.17	15.46	3.21	4.85	3.06	11.12
Vertical transport	5.99	2.30	0.23	8.52	7.18	3.36	1.35	11.89	4.09	2.10	0.68	6.87
$\delta K/\delta T$				0.23				0				−0.42
Residual	−1.55	2.16	−1.29	−0.45	−2.31	−0.03	−2.27	−4.61	−0.80	1.45	0.32	0.55

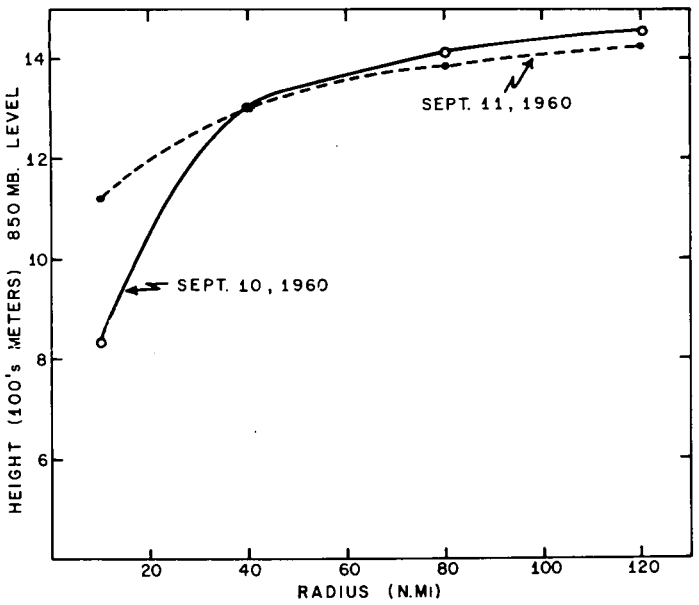

FIGURE 22.—Radial profiles of the height of the 850-mb. surface.

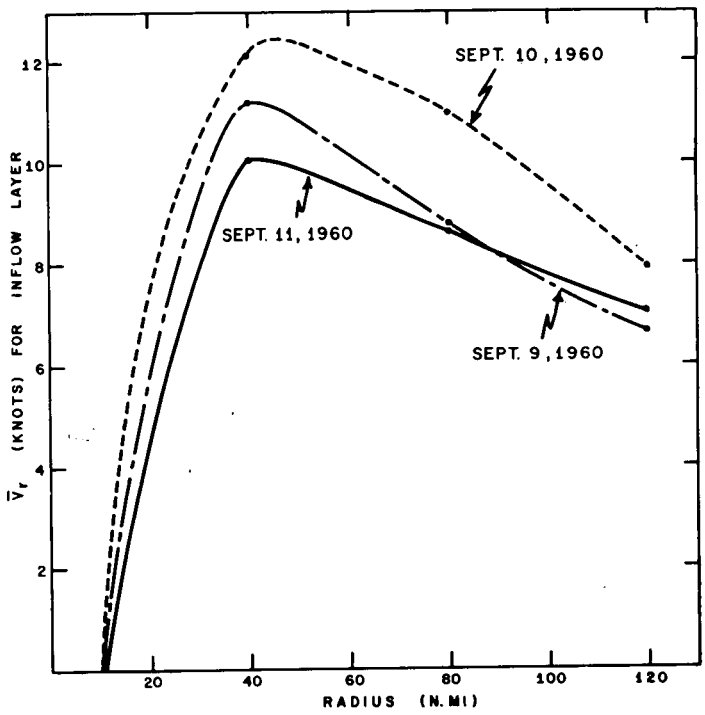

FIGURE 23.—Radial profiles of the vertical mean of the radial wind for the inflow layer.

circulation of the inflow layer itself must have been weakening.

Reduced production of kinetic energy after landfall resulted from a decrease in the pressure gradients and not primarily from a reduction in the mass flow. This may be seen from an examination of figures 22 and 23. The former shows representative curves of the 850-mb. surface on each of two days. The latter shows the radial mean wind for the inflow layer; the mean v_r on the 11th is about 80 percent of its value on the 10th. Since production within the 10–120-n. mi. area decreased about 50 percent, it is apparent that this decrease was not due to a reduction in the mass flow. It has already been shown that the pressure gradients decreased because the core cooled, and that this cooling was due to a removal of the oceanic heat source. Hence, one may conclude that the circulation of the inflow layer also weakened because the surface heat source was removed.

6. SUMMARY AND CONCLUSIONS

As air flows toward the center of a tropical cyclone over the oceans, sensible and latent heat is added along the trajectory. These additions raise the equivalent potential temperature of the air, and a radial gradient of equivalent potential temperature is produced at the surface. As air ascends at different radii a radial gradient of mean virtual temperature from the surface to the upper troposphere results. This warm core structure is responsible for the intense pressure gradients found in tropical cyclones.

Over land, however, a horizontal trajectory takes a path which is very close to moist adiabatic. The oceanic heat source is absent, and the resultant radial gradient of equivalent potential temperature at the surface is destroyed or greatly weakened. Following ascent of this surface air, the gradient of mean virtual temperature from the surface to the upper troposphere is destroyed. The warm air that was previously concentrated near the core of the cyclone is spread out over the larger area. The pressure in the interior rises; at the same time, the pressure at some outer radii (in Donna this was outside the 40-n. mi. radius) falls. This cooling of the core of the cyclone eventually results in weakening and decay of the circulation.

Mass flow through the inflow layer remained virtually unchanged after the cyclone moved inland, at least for a period of several hours. However, within a few hours, the radial gradients of the heights of the constant pressure surfaces near the core of the cyclone decreased to less than one-half their value at the time of landfall. The production of kinetic energy is proportional to the product of the mass flow and the height gradients. Hence, the production of kinetic energy decreased. Since height gradients are known to depend upon thermal gradients, and since the decrease in the height gradients was due to cooling of the core of the cyclone, it follows that the decrease in the production of kinetic energy was due to cooling of the interior of the cyclone.

The surface drag coefficients are larger over land than they are over water by a factor of a little over two. The dissipation of kinetic energy by surface friction is proportional to the product of the drag coefficient and the third power of the surface wind speed. The increased

surface roughness over land results in a decrease in the surface wind speed. Turbulence theory suggests that there must also be greater vertical shear over land than over water, i.e., the decrease in the wind at the anemometer level is greater than it is at some higher level, say 100 m. This, however, cannot be verified with the data available. It can be shown, however, that within a few hours after landfall the dissipation of kinetic energy by surface friction is less over land than it is over water.

With all these factors considered, it is concluded that hurricane Donna filled and weakened over land as a result of the removal of the oceanic heat source. Increased surface roughness over land resulted in some reduction in the surface wind speed, but was not responsible for the filling of the cyclone.

ACKNOWLEDGMENTS

The author is indebted to Professors Herbert Riehl and Sverre Petterssen for encouragement, advice, and many helpful suggestions throughout the course of this research.

REFERENCES

1. T. Bergeron, "The Problem of Tropical Hurricanes," *Quarterly Journal of the Royal Meteorological Society*, vol. 80, No. 344, Apr. 1954, pp. 131–164.
2. H. R. Byers, *General Meteorology*, McGraw-Hill Book Co., Inc., New York, 1959, 540 pp. (p. 392).
3. E. L. Deacon and W. C. Swinbank, "Comparison between Momentum and Water Vapor Transfer," Paper No. 2, Arid Zone Climatology, Australian-UNESCO Symposium, 1956.
4. C. E. Deppermann, *Some Characteristics of Philippine Typhoons*, Weather Bureau, Manila, P.I., 1939, 128 pp.
5. E. L. Fisher, "Hurricanes and the Sea Surface Temperature Field," *Journal of Meteorology*, vol. 15, No. 3, June 1958, pp. 328–333.
6. W. M. Gray, "On the Scale of Motion and Internal Stress Characteristics of the Hurricane," Unpublished manuscript, Department of Atmospheric Science, Colorado State University, Ft. Collins, Colo., 1963.
7. B. Haurwitz, *Dynamic Meteorology*, McGraw-Hill Book Co., Inc., New York and London, 1941, 365 pp. (p. 55).
8. H. F. Hawkins, "Vertical Wind Profiles in Hurricanes," *National Hurricane Research Project Report* No. 55, U.S. Weather Bureau, 1962, 16 pp.
9. L. F. Hubert, "Frictional Filling of Hurricanes," *Bulletin of the American Meteorological Society*, vol. 36, No. 9, Nov. 1955, pp. 440–445.
10. L. A. Hughes, "On the Low-Level Wind Structure of Tropica, Cyclones," *Journal of Meteorology*, vol. 9, No. 6, Dec. 19521 pp. 422–428.
11. W. C. Jacobs, "On the Energy Exchange Between Sea and Atmosphere," *Journal of Marine Research*, vol. 5, 1942, pp. 37–66.
12. E. S. Jordan, "An Observational Study of the Upper Wind Circulation around Tropical Storms," *Journal of Meteorology*, vol. 9, No. 5, Oct. 1952, pp. 340–346.
13. D. W. Krueger, "A Relation between the Mass Circulation through Hurricanes and Their Intensity," *Bulletin of the American Meteorological Society*, vol. 40, No. 4, Apr. 1959, pp. 182–189.
14. J. Malkus and H. Riehl, "On the Dynamics and Energy Transformations in Steady-State Hurricanes," *National Hurricane Research Project Report* No. 31, U.S. Weather Bureau, 1959, 31 pp.
15. J. Malkus and H. Riehl, "Some Aspects of Hurricane Daisy, 1958," *National Hurricane Research Project Report* No. 46, U.S. Weather Bureau, 1961, 64 pp.
16. B. I. Miller, "The Three-Dimensional Wind Structure around a Tropical Cyclone," *National Hurricane Research Project Report* No. 15, U.S. Weather Bureau, 1958, 41 pp.
17. B. I. Miller, "Rainfall Rates in Florida Hurricanes," *Monthly Weather Review*, vol. 86, No. 7, July 1958, pp. 258–264.
18. B. I. Miller, "On the Energy and Momentum Balance of Hurricane Helene (1958)," *National Hurricane Research Project Report* No. 53, U.S. Weather Bureau, 1962, 19 pp.
19. E. Palmén, "On the Formation and Structure of Tropical Hurricanes," *Geophysica*, vol. 3, 1948, pp. 26–38.
20. E. Palmén, "Formation and Development of Tropical Cyclones," *Proceedings of the Tropical Cyclone Symposium*, Brisbane, Dec. 1956, pp. 212–231.
21. E. Palmén and H. Riehl, "Budget of Angular Momentum and Energy in Tropical Cyclones," *Journal of Meteorology*, vol. 14, No. 2, Apr. 1957, pp. 150–159.
22. S. Petterssen, *Weather Analysis and Forecasting*, McGraw-Hill Book Co., Inc., New York and London, 428 pp. (pp. 27–29).
23. S. Petterssen, D. L. Bradbury, and K. Pedersen, "Heat Exchange and Cyclone Development on the North Atlantic Ocean," The University of Chicago, Department of the Geophysical Sciences, 1961, 76 pp.
24. A. C. Pike, "The Oceanic Heat Budget as Affected by Hurricane Audrey (1957)," Civil Engineering Department, Colorado State University, Ft. Collins, 1962, 7 pp.
25. C. H. B. Priestley, *Turbulent Transfer in the Lower Atmosphere*, University of Chicago Press, Chicago, Ill., 1959, 130 pp. (p. 93).
26. N. E. Rider, "Eddy Diffusion of Momentum, Water Vapour, and Heat Near the Ground," *Philosophical Transactions of the Royal Society of London*, Series A, vol. 246, 1954, pp. 481–501.
27. H. Riehl, T. C. Yeh, J. S. Malkus, and N. E. LaSeur, "The Northeast Trades of the Pacific Ocean," *Quarterly Journal of the Royal Meteorological Society*, vol. 77, 1951, pp. 598–626.
28. H. Riehl, *Tropical Meteorology*, McGraw-Hill Book Co., Inc., New York and London, 392 pp. (pp. 341, 300).
29. H. Riehl, "On the Production of Kinetic Energy from Condensation Heating," *The Atmosphere and the Sea in Motion* (Rossby Memorial Volume), The Rockefeller Institute Press and Oxford University Press, New York, 1959, pp. 381–399.
30. S. L. Rosenthal, "Concerning the Mechanics and Thermodynamics of the Inflow Layer of the Mature Hurricane," *National Hurricane Research Project Report* No. 47, U.S. Weather Bureau, 1961, 31 pp.
31. S. L. Rosenthal, "Some Attempts To Simulate the Development of Tropical Cyclones by Numerical Methods," *Monthly Weather Review*, vol. 92, No. 1, Jan. 1964, pp. 1–21.
32. P. A. Sheppard, "Transfer Across the Earth's Surface and Through the Air Beyond," *Quarterly Journal of the Royal Meteorological Society*, vol. 84, No. 361, July 1958, pp. 205–224.
33. H. U. Sverdrup, "Oceanography," *Handbuch der Physik*, Springer-Verlag, Berlin, 1957, pp. 608–670.
34. C. W. Thornthwaite and B. Holzman, "The Determination of Evaporation from Land and Water Surfaces," *Monthly Weather Review*, vol. 67, No. 1, Jan. 1939, pp. 4–11.
35. B. W. Wilson, "Note on Surface Wind Stress over Water at Low and High Wind Speeds," *Journal of Geophysical Research*, vol. 65, No. 10, Oct. 1960, pp. 3377–3382.

[*Received April 13, 1964*]